



Wall-to-bed heat transfer in vertical hydraulic transport and in particulate fluidized beds

Radmila Garić-Grulović^{a,*}, Nevenka Bošković-Vragolović^b, Željko Grbavčić^b, Zorana Arsenijević^a

^a Institute for Chemistry, Technology and Metallurgy, University of Belgrade, Njegoševa 12, 11000 Belgrade, Serbia

^b Faculty of Technology and Metallurgy, Department of Chemical Engineering, University of Belgrade, Karnegijeva 4, 11000 Belgrade, Serbia

ARTICLE INFO

Article history:

Received 28 November 2007

Available online 3 July 2008

Keywords:

Liquid–solids

Heat transfer

Vertical transport

Fluidized bed

Pseudofluid

ABSTRACT

Wall-to-bed heat transfer in hydraulic transport and in particulate fluidized beds of spherical particles was studied. Experiments were performed by spherical glass particles of 0.80–2.98 mm in diameter with water in a 25.4 mm I.D. cooper tube equipped with a steam jacket.

In the hydraulic transport runs the Reynolds number varied between 3300 and 20150 (particles of 1.20, 1.94 and 2.98 mm in diameter), while in particulate fluidized beds Reynolds number varied between 1960 and 7850 (particles of 0.80, 1.10 and 1.94 mm in diameter). The influence of different parameters as liquid velocity, particles size and voidage on heat transfer in fluidized beds and in hydraulic transport are presented.

In our hydraulic transport experiments, the two characteristic flow regimes were observed: “turbulent” and “parallel” flow. Our experimental data show that the heat transfer coefficients in “turbulent” regime are much higher than in “parallel” flow, and the heat transfer coefficients is generally higher while the flow is in fluidized bed.

The data for heat transfer in particulate fluidized beds and for vertical hydraulic transport were correlated treating the flowing fluid–particle mixture as a pseudo fluid. New correlation for heat transfer factor in fluidized beds and in vertical hydraulic transport is proposed.

© 2008 Elsevier Ltd. All rights reserved.

1. Introduction

Numerous industrial applications of liquid–solid systems require transfer characteristics determination and research of heat transfer in liquid–solid systems. Note that, many industrial continuous processing equipment treats a two-phase mixture of solids and fluid such as water treatment, polymerization, biotechnology, food processing, etc. [1–4]. To understand and model heat transfer the temperatures and heat transfer coefficients must be known [5–7].

In the first place, knowledge of heat transfer in liquid–solid contactors is most important for design of heat exchangers [8]. Presence of suspended particles in liquid intensifies transfer due to excellent mixing of the bulk fluid. For liquid–solid fluidized beds Richardson et al. [9] found that heat transfer coefficient are up to 8 times higher than for single phase flow at the same velocity. The same author accentuated that particles in suspension has scouring action because reduce the formation of deposits on the heat transfer surfaces.

The subject of the present investigation was to study the effect of particles on the wall-to-bed heat transfer (fluidized bed and

flowing suspension) and attempt to relate the wall-to-bed heat transfer with the friction between the heating wall and the liquid–solids fluidized bed and flowing suspension.

2. Experimental

The heat transfer experiments were conducted with spherical glass spheres transported (1.20, 1.94, 2.98 mm in diameter) and fluidized (0.80, 1.10, 1.94 mm in diameter) with water. The schematic diagram of the experimental systems is shown in Fig. 1 (A – vertical transport setup; B – fluidization setup).

The transport line (c, Fig. 1) was 27.4/25.4 mm OD/ID, 1360 mm long cooper tube, equipped with a 700 mm long steam jacket. The tube was mounted in a modified spouted bed in order to obtain a non-fluctuating controlled flow of particles. The heating section (d) was located far enough (320 mm) from the inlet to the transport line, where the suspension flow in a non-accelerating i.e., the steady state flow regime during the heat transfer runs. At the bottom of the bed, the water was introduced through the nozzle (a). The separation distance between the bed bottom and the transport tube inlet (L, Fig. 1A) was 20 mm.

The fluid and particle flowrates were measured using a designated box (g). The pressure gradient were measured using piezometers (i). Temperatures were measured with Ni–Cr thermocouples.

* Corresponding author. Tel.: +381 11 3370500; fax: +381 11 3370408.
E-mail address: garic@elab.tmf.bg.ac.yu (R. Garić-Grulović).

Nomenclature

A_t	cross-sectional area of the transport tube (m ²)	Re_p	Reynolds number for particles, $Ud_p\rho_f/\mu$
c_{pf}	specific heat of fluid (J/kg K)	T	temperature (K)
c_{pp}	specific heat of solids (J/kg K)	T_m	the mean logarithmic temperature difference (K)
c_s	particle superficial velocity in the transport tube, $G_p/(\rho_p A_t)$ (m/s)	ΔT_{lm}	the mean temperature (K)
d_p	particle diameter (m)	u	mean interstitial fluid velocity in the transport tube, U/ε (m/s)
D_t	diameter of the transport tube and fluidized bed (m)	U	superficial fluid velocity in the transport tube (m/s)
f_{cf}	collision frequency (s ⁻¹)	U_m	superficial fluid suspension velocity, $(U + c_s)$ (m/s)
f	fluid-wall friction coefficient by Eq. (7), $4f_f$	U_t	particle terminal velocity in an infinite medium (m/s)
f_f	fluid-wall friction coefficient	U_{mF}	minimum fluidization velocity (m/s)
f_p	particle-wall friction coefficient	V	water flowrate at the column inlet (m ³ /s) (Fig. 1)
f_w	suspension-wall friction coefficient	V_A	water flowrate through the moving packed bed (m ³ /s) (Fig. 1)
F_e	pressure gradient due to the effective weight of particles (Pa/m)	V_T	water flowrate through the draft tube (m ³ /s) (Fig. 1)
F_f	pressure gradient due to the fluid-wall friction (Pa/m)	W_p	particle mass flux, G_p/A_t (kg/(m ² s))
F_p	pressure gradient due to the particle-wall friction (Pa/m)	z	vertical coordinate (m)
F_w	pressure gradient due to the suspension-wall friction (Pa/m)	<i>Greek symbols</i>	
g	gravitational acceleration (m/s ²)	α	heat transfer coefficient (kW/(m ² K))
G_f	fluid mass flowrate in the transport tube (kg/s)	γ^*	criterion for regime transition from “turbulent” to the “parallel”
G_p	particle mass flowrate in the transport tube (kg/s)	ε	averaged voidage in the transport tube
j_D	mass transfer factor	ε_{mF}	voidage at minimum fluidization
j_H	heat transfer factor, $\alpha/(\rho_f c_{pf} U) Pr^{2/3} = Nu/(Re Pr^{1/3})$	ε_{SB}	voidage in static bed
L	separation distance between the inlet nozzle and the transport tube inlet (see Fig. 1) (m)	λ	water thermal conductivity (W/(mK))
L_H	length of heating zone (m)	μ	viscosity of the fluid (Ns/m ²)
Nu	Nusselt number, $\alpha D_t/\lambda$	μ_m	viscosity of the fluid-particle suspension (Ns/m ²)
Pr	Prandtl number, $\mu c_{pf}/\lambda$	μ_w	viscosity of the fluid on the wall of the tube (Ns/m ²)
Re	Reynolds number, $D_t \rho_f U/\mu$	ρ_f	fluid density (kg/m ³)
Re_m	modified suspension Reynolds number, $D_t \rho_m U_m/\mu_m$	ρ_p	particle density (kg/m ³)
		ρ_m	average suspension density, $(\varepsilon \rho_f + (1 - \varepsilon) \rho_p)$ (kg/m ³)

The wall temperature were measured at two points (inlet and exit of the heating zone), on a such way that junction point was filled with tin at about 0.2 mm from the inside tube wall, as shown schematically on Fig. 1 (detail “A”). The temperature of the fluid-particle suspension was measured by a thermocouple located in the tube axis. It was assumed that at the inlet and at the outlet of the heating zone, the particles and the fluid have the same temperature. The heat transfer coefficient is given by:

$$\alpha = \frac{(G_f c_{pf} - G_p c_{pp})(T_2 - T_1)}{(D_t \pi L_H) \Delta T_{lm}} \quad (1)$$

The fluidization experiments were conducted in the same experimental system as shown in Fig. 1A. The only difference was that transport tube was replaced by a fluidization column with the same diameter and the same heat transfer area. The heat transfer coefficient at fluidized beds was calculated as:

$$\alpha = \frac{G_f c_{pf}(T_2 - T_1)}{(D_t \pi L_H) \Delta T_{lm}} \quad (2)$$

The mean logarithmic temperature difference in above Eqs. (1) and (2) is defined as:

$$\Delta T_{lm} = \frac{(T_4 - T_1) - (T_3 - T_2)}{\ln \frac{(T_4 - T_1)}{(T_3 - T_2)}} \quad (3)$$

A total of 68 data points were collected in the hydraulic transport runs, and a total of 159 data points on heat transfer coefficients were collected during fluidized beds runs. Particle characteristics and the range of experimental conditions are shown in Table 1.

The physical characteristics of water were determined for the mean temperature:

$$T_m = \frac{T_1 + T_2}{2} \quad (4)$$

Table 1
Particle characteristics and range of experimental conditions

	Hydraulic transport			Fluidized beds		
d_p (mm)	1.20	1.94	2.98	0.80	1.10	1.94
ρ_p (kg/m ³)	2641	2507	2509	2923	2641	2507
U_{mF} (m/s)	0.0120	0.0205	0.0310	0.0083		0.0205
U_t (m/s)	0.1884	0.2878	0.3698	0.1154	0.2200	0.2878
U/U_t	0.43–2.15	0.31–2.86	0.29–2.11			
G_p/G_f	0.08–0.24	0.08–0.30	0.07–0.33	–	–	–
W_p (kg/m ² s)	6.5–86.9	0.7–226.2	6.0–239.3	–	–	–
ε_{mF}	0.420	0.447	0.462	0.398	0.400	0.447
ε_{calc}	0.78–0.90	0.75–0.88	0.72–0.86	0.69–0.92	0.65–0.92	0.50–0.97

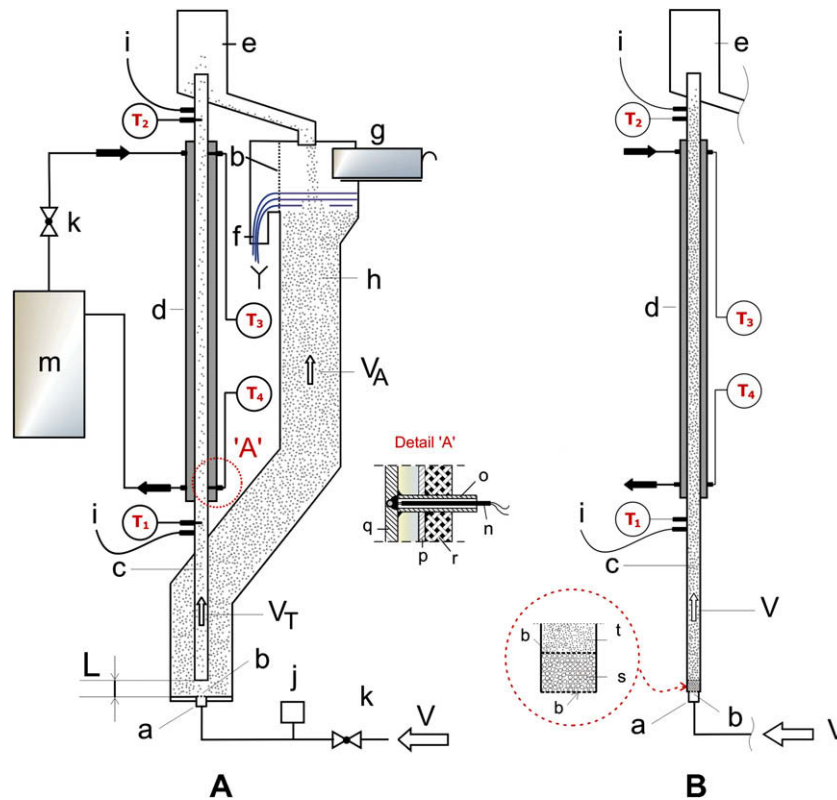


Fig. 1. Schematic diagram of experimental systems: (A) Vertical transport setup; (B) Fluidization setup; (a) – inlet nozzle, 20 mm i.d., (b) – screen, (c) – transport tube, 25.4 mm i.d., (d) – heating section, 700 mm in length, (e) – overflow, (f) – water overflow, (g) – box, (h) – modified spouted bed, 70 × 70 mm in cross-section, (i) – pressure taps, (j) – flowmeter, (k) – valve, (l) – distance of 20 mm, (m) – steam generator, 30 kW, (s) – distributor, (t) – fluidized bed, (n) – Ni-Cr thermocouple, (o) – cooper tube 8/6 mm, (p) – jacket wall, (q) – transport tube wall, (r) – thermoinsulation.

3. Results and discussion

3.1. Two-phase flow and fluidized bed

The effect of superficial liquid phase velocity U , on wall-to-bed heat transfer coefficient α , in fluidized bed and two-phase flow (hydraulic transport) is shown in Fig. 2. As can be seen, α exhibits its maximum value with a variation of U in fluidized bed. In the relatively lower range of U , turbulence intensity in the bed increases with increasing U . However turbulence intensity decreases with a further increase in U due to the reduction of solids holdup in the bed. The presence of particles improves the heat transfer for lower liquid phase velocity, where the particles concentration in solid-liquid suspension, i.e. in fluidized bed, is generally higher than in hydraulic transport.

The effect of particle size on the heat transfer coefficient also is shown in Fig. 2. As can be seen, heat transfer coefficient increases with increasing particle size in all studied cases. The boundary layer around the heater surface can be effectively eroded to decrease the heat transfer resistance in the beds of relatively larger particles, with a consequent increase in heat transfer with increasing particle size [10].

Since the bed porosity is a proportional function of superficial fluid velocity U in fluidized beds, the variation of α with U is very similar to that with bed porosity, as can be seen in Fig. 3. The maximum value of α with respect to the fluidized bed porosity can be attributed to the variation of effective turbulence related to solid phase holdup in the beds. The turbulence intensity attains its optimum value for heat transfer at the intermediate bed porosity and the corresponding continuous liquid phase velocity conditions. The bed porosity at which α exhibits its maximum value decreases with increasing particle size in liquid fluidized beds since minimum fluidization velocity (U_{mf}) increases with increasing particle size.

Brea and Hamilton [11] explain the shape of the α - U plot for liquid-solid fluidized beds as influence of particles on boundary layer. Motion of the solid particles disturb the laminar sub-layer at the heating surface. On the other side, higher liquid velocity causes a less concentration of particles and the possibility of the disturbance is less. These are two opposing effects on heat transfer lead to the maximum for the heat transfer.

Aghajani et al. [8] introduced the collision frequency of contacting particles in the bed:

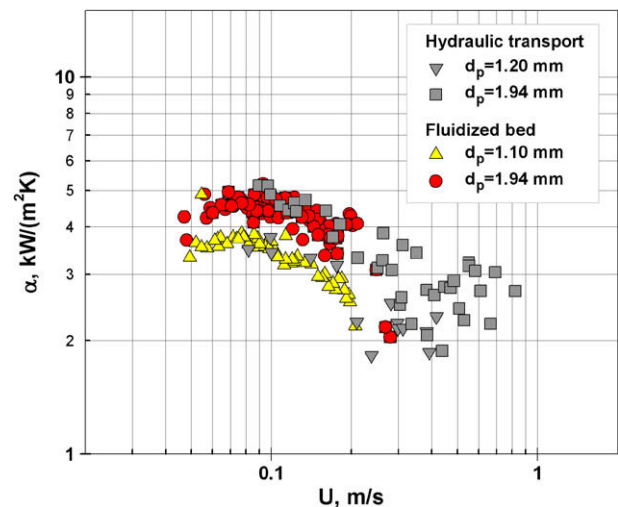


Fig. 2. Heat transfer coefficient, α vs. U for hydraulic transport and fluidized bed.

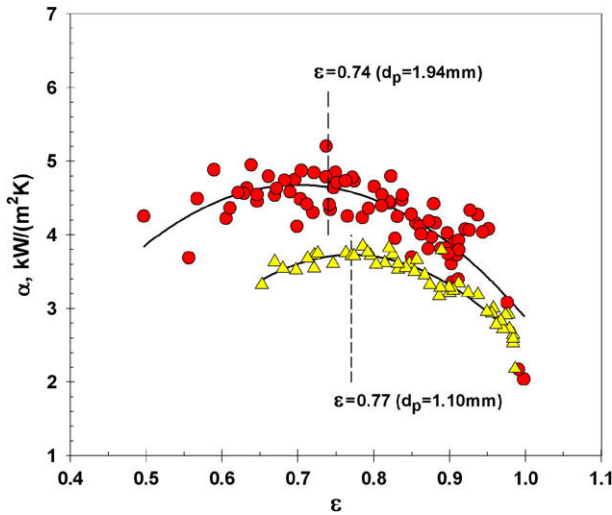


Fig. 3. Heat transfer coefficient, α , vs. ϵ for fluidized bed ($d_p = 1.94$ mm).

$$f_{cf} = 1.5 \frac{U}{d_p} (1 - \epsilon)^{1.8} (\epsilon - \epsilon_{SB})^{0.2} \quad (5)$$

The collision frequency of contacting particles with heat transfer surfaces increases from zero for a packed bed up to a maximum value at some bed voidage and decreasing to zero for single phase flow. The shape of the f - ϵ plot is the same as the shape of the α - ϵ plot.

The influence of particle in flow on heat transfer can be seen in Fig. 4. The data for Nusselt number presented as a function of the Reynolds number for fluidized beds, vertical transport and single phase flow. The presence of particles intensifies heat transfer for Reynolds number less than 10000, where is the particles concentration in flowing mixture generally higher. The heat transfer in fluidized bed increases relative to the values in single phase flow by a factor of about 2.2. For higher Reynolds number (approximately $Re > 10000$) there is no significant difference in heat transfer between single phase flow and hydraulic transport.

A comparison of the experimental data for the single phase flow with several literature correlations are also shown in Fig. 4.

The Dittus–Boelter [12] heat transfer correlation for turbulent flow ($Re > 10000$) is:

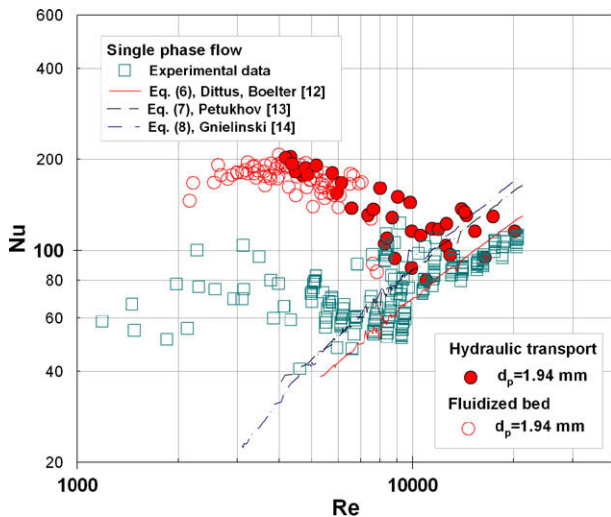


Fig. 4. Relationship of Nu vs. Re for suspension flow (hydraulic transport) and liquid fluidized bed, $d_p = 1.94$ mm.

$$Nu = 0.023 \cdot Re^{0.8} \cdot Pr^{1/3} \quad (6)$$

The predicted values from the correlation (6), have shown good agreement with our experimental data.

An correlation for the heat transfer in smooth straight tubes is proposed by Petukhov [13] ($0.5 < Pr < 200$, $10^4 < Re < 10^6$ and $0.8 < (\mu/\mu_w) < 40$)

$$Nu = \frac{\left(\frac{f}{8}\right) Re \cdot Pr}{1.07 + 12.7 \cdot \left(\frac{f}{8}\right)^{1/2} \cdot (Pr^{2/3} - 1)} \left(\frac{\mu}{\mu_w}\right)^n \quad (7)$$

Besides, Gnielinski [14] proposed following correlation for heat transfer, also in smooth straight tubes, recommended in the following range of variables: $0 < D_i/L_H < 1$, $0.6 < Pr < 2000$ and $2300 < Re < 10^6$,

$$Nu = \frac{\frac{f}{8} (Re - 1000) \cdot Pr}{1 + 12.7 \cdot \sqrt{\frac{f}{8}} \cdot (Pr^{2/3} - 1)} \left[1 + \left(\frac{D_t}{L_H}\right)^{2/3}\right] \quad (8)$$

where in Eqs. (7) and (8), the fluid-wall friction coefficient is given by the following correlation

$$f = [1.82 \cdot \log(Re) - 1.64]^{-2} \quad (9)$$

Eqs. (7) and (8) represents the majority of the data within 20%.

However, in the transition regime ($2300 < Re < 10000$) there is significant difference between available correlations and our data, and the heat transfer results in the transition regime are uncertain because of the large number of parameters which determine when and how transition occurs.

The heat transfer factor as a function of Reynolds number of particles for fluidized beds and hydraulic transport is shown in Fig. 5. As can be seen, the fluidized bed and the vertical transport data overlap for $300 \leq Re_p \leq 600$ because the concentration of particles in these systems is nearly the same. Note that in our investigations we are noticed that vertical two-phase flow begins at the maximum value on heat transfer coefficient (Fig. 2), i.e. when fluidized bed porosity is corresponding with continuous solid-liquid phase conditions. At the same time, the flowing mixture is very much like a particularly fluidized bed, where the whole “fluidized” mixture flows relative to the tube walls.

Comparison of the data for heat transfer in fluidized bed ($d_p = 1.94$ mm) with several literature correlations also is presented in Fig. 5.

Muroyama et al. [15] proposed the following correlation for heat transfer in fluidized bed:

$$j_H \epsilon = 0.137 Re_p^{-0.271} \quad (10)$$

where $Re'_p = Re_p / (1 - \epsilon)$, in the following range of variables: $11 < Re'_p < 2620$; $Pr = 4.3 - 135.5$; $0.495 < \epsilon < 0.95$.

Also, Kang et al. [16] have given the correlation for heat transfer in fluidized bed:

$$j_H \epsilon = 0.191 Re_p^{-0.31} \quad (11)$$

The Eq. (11) is recommended in the following range of variables: $68 < Re_p < 480$; $Pr = 5.6$; $0.50 < \epsilon < 0$. The data calculated with correlation (10) and (11) show good agreement with our experimental data.

For the heat transfer in liquid fluidized bed Bošković proposed experimental correlation [17]:

$$j_H \epsilon = 0.17 Re_p^{-0.3} \quad (12)$$

This correlation was developed using the same spherical glass particles ($d_p = 0.8 - 3$ mm) and the same experimental system shown in Fig. 1B.

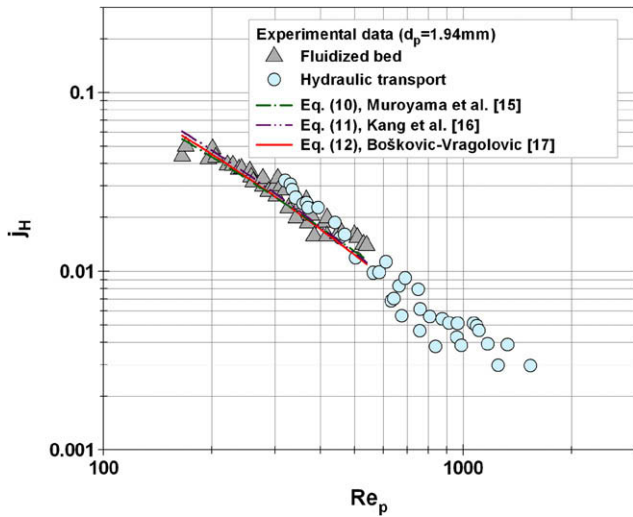


Fig. 5. Heat transfer factor, j_H , vs. Re_p for hydraulic transport and fluidized bed ($d_p = 1.94$ mm).

It can be noticed that correlations (10)–(12) involve effect of voidage through the group $j_H \cdot \varepsilon$ and $Re'_p = Re_p / (1 - \varepsilon)$.

Relationship between the heat transfer factor and the bed voidage is shown in Fig. 6. It can be seen that the fluidized bed data and the vertical transport data overlap for small range of bed voidage ($0.74 < \varepsilon < 0.77$). For $\varepsilon > 0.77$ data differs significantly for those systems. It's interesting that for $\varepsilon > 0.77$, for the same fluid velocity, concentration of particles in fluidized beds is smaller than in vertical transport. That means that beside fluid velocity and particles concentration, particles movement and fluid mixing caused by particles also have large impact on heat transfer. For higher liquid velocities at hydro-transport, particles are moving with small radial movement causing lower intensity of fluid mixing and because of that heat transfer is lower for all particles concentration.

3.1.1. Flow regime

In hydraulic transport of coarse particles, we have observed two characteristic flow regimes:

- “Turbulent” flow where the particles move vertically but with noticeable radial movement. This regime is characteristic of the lower fluid and particle velocities.

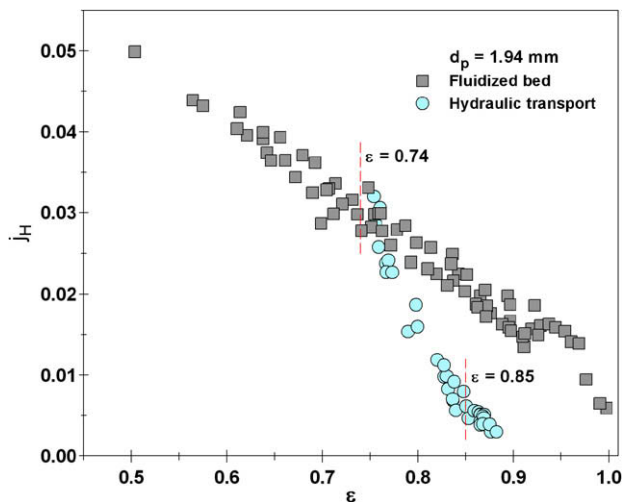


Fig. 6. Heat transfer factor, j_H , vs. ε for fluidized bed and hydraulic transport ($d_p = 1.94$ mm).

- “Parallel” flow where the particles move vertically along parallel streamlines. This regime is characteristic of the higher fluid and particle velocities.

In Fig. 7 is presented schematic illustration of particle movement in fluidized bed and hydraulic transport. Particles in fluidized beds move randomly at all direction (Fig. 7a) and net particle flowrate G_p is zero. “Turbulent” flow in hydro-transport is similar to the particulate fluidized beds (Fig. 7b). Particles move vertically with radial movements and certainly $G_p \neq 0$. In “parallel” flow particles move vertically without radial movement (Fig. 7c).

In our previous work [21] criterion for regime designation in the hydraulic transport of coarse particles is present. It is parameter γ derived from the steady state one-dimensional suspension momentum equation [21]:

$$-\frac{dp}{dz} = (\rho_p - \rho_f)g(1 - \varepsilon) + F_w + \gamma \frac{d\varepsilon}{dz}$$

where

$$\gamma = \rho_p v^2 - \rho_f u^2$$

Dimensionless form of this parameter is γ^*

$$\gamma^* = \frac{\rho_p v^2 - \rho_f u^2}{\rho_f U_t^2}$$

Our visual observations indicate that $\gamma = 0$ or $\gamma^* = 0$ in hydraulic transport corresponds to the transient form “turbulent” to “parallel” flow. For particulate fluidized beds always is $\gamma < 0$.

The data given in Fig. 8 indicate much higher heat transfer between the flowing suspension and tube wall in the “turbulent” flow regime. Since in the “turbulent” flow regime the frequency of particle collisions with the tube wall is much higher, it is reasonable to expect higher heat transfer rate in this flow regime. Fig. 8 shows that this is indeed the case, since heat transfer factors rapidly increase when $\gamma^* < 0$.

3.1.2. Momentum and heat transfer in vertical liquid–solids flow and fluidized beds

The one-dimensional suspension momentum balance outside acceleration zone in vertical liquid–solids flow, through the transport tube is [18,19]:

$$-\frac{dP}{dz} = (\rho_p - \rho_f)g(1 - \varepsilon) + F_p + F_f \quad (13)$$

In Eq. (13) overall pressure gradient ($-dP/dz$), that can be obtained only experimentally, is sum of effective weight of the suspension $(\rho_p - \rho_f)g(1 - \varepsilon)$, pressure gradient due to the particle-wall, F_p and fluid-wall friction, F_f . Those friction terms represent overall suspension-wall friction:

$$F_w = F_p + F_f \quad (14)$$

The pressure gradients due to particle-wall and fluid-wall friction written in terms of friction factors f_p and f_f [19], are

$$F_p = 2f_p \rho_p \frac{(1 - \varepsilon)v^2}{D_t} \quad (15)$$

$$F_f = 2f_f \rho_f \frac{U^2}{D_t} \quad (16)$$

Also, in fluidized beds momentum transfer is defined by Eq. (13) and it is equal to the effective weight of the suspension $(\rho_p - \rho_f)g(1 - \varepsilon)$, according to definition of fluidized bed where $v = 0$, $F_p = 0$ and $F_f = 0$.

Using experimental data for $(-dP/dz)$, U and ε , collected in our previous work in vertical liquid–solids flow [19], the experimental value of F_w was determined by Eq. (13).

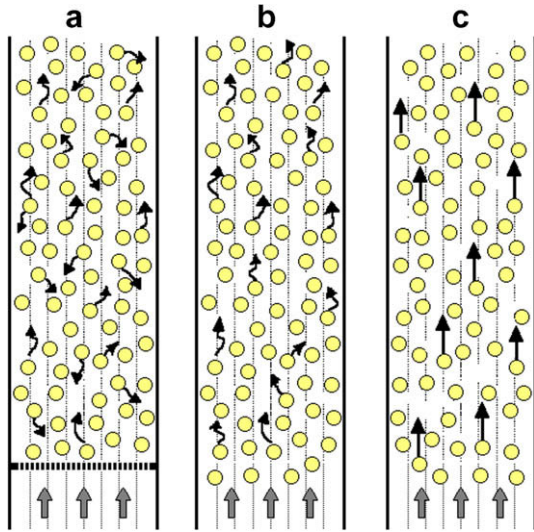


Fig. 7. Schematic illustration of particle movement: (a) fluidized bed, (b) hydraulic transport ("turbulent flow"), (c) hydraulic transport ("parallel flow").

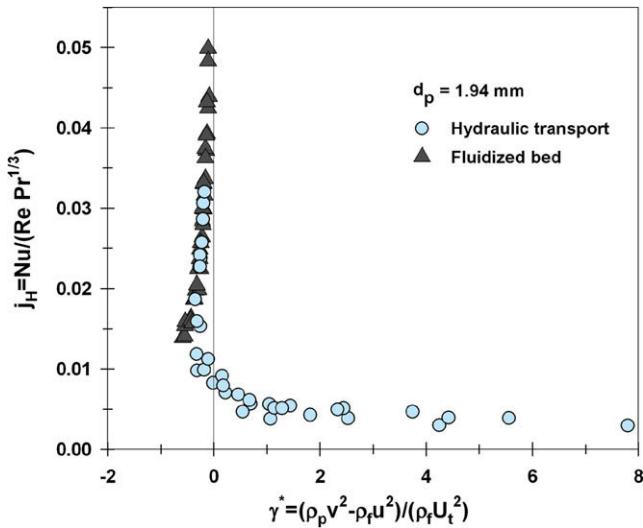


Fig. 8. Effect of the flow regime parameter γ^* on the heat transfer factor j_H .

Treating a flowing suspension in vertical liquid–solids flow as a pseudofluid with the mean density,

$$\rho_m = \varepsilon \rho_f + (1 - \varepsilon) \rho_p \quad (17)$$

a modified suspension–wall friction coefficient can be defined in analogy with Eq. (16):

$$f_w = \frac{F_w D_t}{2 \rho_m U_m^2} \quad (18)$$

where the mean suspension superficial velocity is

$$U_m = U + c_s = \frac{G_f}{\rho_f A_t} + \frac{G_p}{\rho_p A_t} \quad (19)$$

Near the heat transfer area (column wall) in fluidized bed flows fluid which is mixed by particles, but in vertical transport flows fluid–particles suspension. Because of that, superficial fluid suspension velocity ($U_m = U + c_s$) are introduced in analysis of investigated systems. In fluidized bed superficial suspension velocity is equal to the superficial fluid velocity. Fig. 9 shows relationship between the heat transfer factor (j_H) and the superficial suspension velocity (U_m).

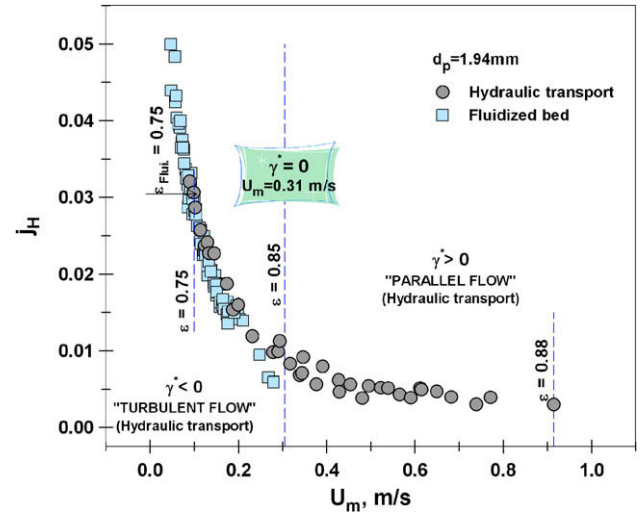


Fig. 9. Relationship of j_H vs. U_m for hydraulic transport and liquid fluidized bed.

"Turbulent" flow regime appears very much like a particulate fluidized bed, therefore it could be expected similar values of j_H factors for "turbulent" hydro-transport and particulate fluidization. Fig. 9 shows that this is really the case. Heat transfer factors for same particles fluidized by water or transported by water in the "turbulent" regime are practically identical.

For the flowing suspension the modified Reynolds number is:

$$Re_m = \frac{D_t \rho_m U_m}{\mu_m} \quad (20)$$

where the effective flowing suspension viscosity is [20]:

$$\mu_m = \mu \cdot \exp\left(\frac{5(1 - \varepsilon)}{3\varepsilon}\right) \quad (21)$$

The experimental data of j_H and experimental data of $f_w/2$ for vertical liquid–solids flow and fluidized bed are plotted in Fig. 10. In the range where the fluidized bed and the vertical transport data overlap ($\varepsilon \geq 0.74$ for $d_p = 1.94$ mm, Fig. 3), i.e. where the concentration of particles in these systems is nearly the same, the data of j_H and $f_w/2$ are practically following the line (Fig. 10).

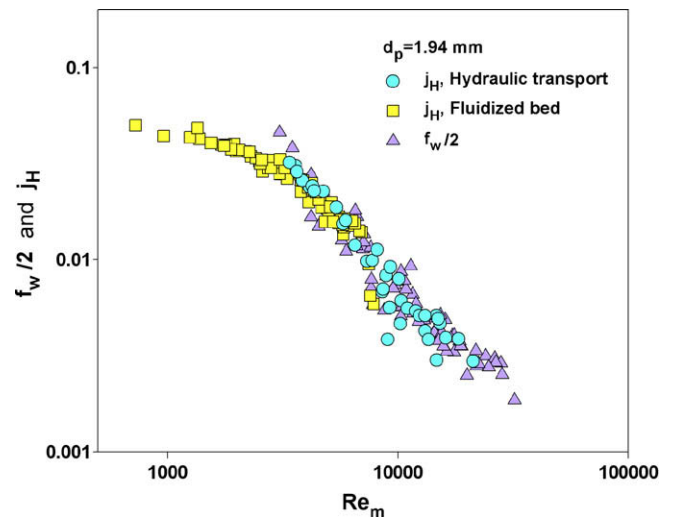


Fig. 10. Relationship of the data for f_w and j_H in hydraulic transport and fluidized beds.

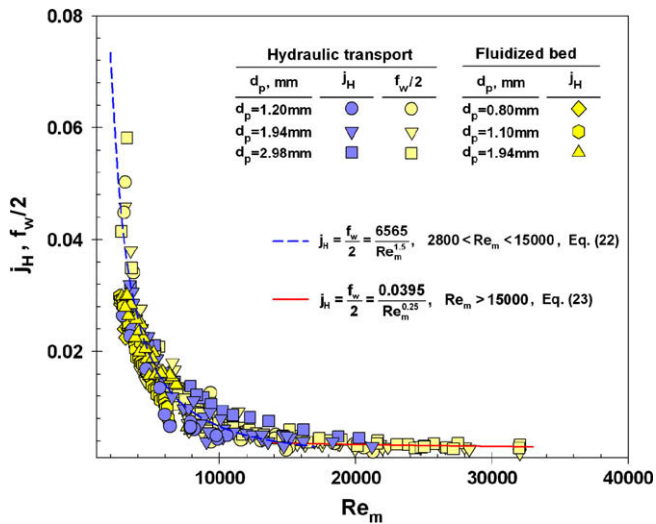


Fig. 11. Correlation of the data for f_w and j_H in suspension flow (hydraulic transport) and fluidized beds for all investigated particles.

Over the range of investigated conditions experimental values of j_H for vertical liquid–solids flow and fluidized bed, and experimental values of $f_w/2$ for vertical liquid–solids flow are presented in Fig. 11, and practically the same. Note that in Fig. 11, all of the presented results for fluidized bed are the data where the concentration of particles are nearly to the values in vertical liquid solids flow ($\varepsilon \geq 0.80$ for $d_p = 0.80$ mm; $\varepsilon \geq 0.77$ for $d_p = 1.1$ and 1.2 mm; $\varepsilon \geq 0.74$ for $d_p = 1.94$ mm). In that range of a concentration in the fluidized bed, the flowing mixture is very much like a particulate fluidized bed, where the whole “fluidized” mixture flows relative to the tube walls, and two systems can be compared (Fig. 11). Presented data for vertical liquid–solids flow and fluidized bed are in good agreement with following equations

$$j_H = f_w/2 = 6565/Re_m^{0.25}, 2800 < Re_m < 15000 \quad (22)$$

and

$$j_H = f_w/2 = 0.0395/Re_m^{0.25}, 15000 < Re_m < 32000 \quad (23)$$

correlated by the vertical liquid–solids flow in our previous work [21]. These Eqs. (22) and (23) are developed on the bases of the Colburn’s j_H -factor [22]. As can be seen, these values of j_H and $f_w/2$ are practically the same in the presented range of investigation, clearly indicating an analogy between the two phenomena.

4. Conclusions

Heat transfer in hydraulic transport of coarse spherical glass particles and in fluidized beds was experimentally studied.

- In the hydraulic transport of coarse spherical glass particles, two characteristic flow regimes were observed: “parallel” and “turbulent” flow regime. Parameter γ^* appears as a criterion for the regime distinction. In “turbulent” flow regime ($\gamma^* < 0$), the heat transfer coefficients are significantly higher than the corresponding values in “parallel” flow. Also, the data of fluidized bed are in the “turbulent” flow regime.
- In the fluidized bed heat transfer coefficient α exhibits its maximum value with a variation of U . Note that the bed porosity ε at

which α exhibits its maximum value. In the relatively lower range of U , turbulence intensity in the bed increases with increasing U , however turbulence intensity decreases with a further increase in U due to the reduction of solids holdup in the bed.

- Heat transfer factors for same particles fluidized by water or transported by water in the “turbulent” regime are practically identical.
- The data for wall-to-bed heat transfer in hydraulic transport of coarse spherical glass particles and in fluidized beds in certain range of investigation ($\varepsilon \geq 0.80$ for $d_p = 0.80$ mm; $\varepsilon \geq 0.77$ for $d_p = 1.1$ and 1.2 mm; $\varepsilon \geq 0.74$ for $d_p = 1.94$ mm), show that an analogy between heat and momentum transfer exists.

Acknowledgement

Financial support of the Research Council of Serbia is gratefully acknowledged.

References

- [1] S. Mankad, K.M. Nixorf, P.J. Fryer, J. Food Eng. 31 (1907) 9–33.
- [2] P.K. Agarwal, Transport phenomena in multiparticle systems II: Particle–fluid heat and mass transfer, Chem. Eng. Sci. 43 (9) (1988) 2501–2510.
- [3] L. Zhang, P.J. Fryer, Food sterilization by electrical heating: sensitivity to process parameters, AIChE 40 (5) (1994) 888–898.
- [4] P.J. Fryer, Electrical resistance heating of foods, in: G. Gould (Ed.), New Methods of Food Preservation, Chapman and Hall, Edinburgh, 1994.
- [5] M. Haid, H. Martin, H. Müller-Steinhagen, Heat transfer to liquid–solid fluidized beds, Chem. Eng. Process 33 (1994) 211–225.
- [6] M. Haid, Correlations for the prediction of heat transfer to liquid–solid fluidized beds, Chem. Eng. Process 36 (1997) 143–147.
- [7] C.L. Briens, M.A. Bergougnou, New model to calculate the choking velocity of monosize and multisize solids in vertical pneumatic transport lines, Can. J. Chem. Eng. 64 (1986) 196–204.
- [8] M. Aghajani, H. Müller-Steinhagen, New design equations for liquid/solid fluidized bed heat exchangers, Chem. Eng. Commun. 13 (1–3) (2005) 1–16.
- [9] J.F. Richardson, M.N. Romani, K.J. Shakiri, Heat transfer from immersed surfaces in liquid fluidized beds, Chem. Eng. Sci. 31 (8) (1976) 619–624.
- [10] S.D. Kim, J.S. Kim, C.H. Nam, S.H. Kim, Y. Kang, Immersed heater-to-bed heat transfer in liquid–liquid–solid fluidized beds, Chem. Eng. Sci. 54 (21) (1999) 5173–5179.
- [11] F.M. Brea, W. Hamilton, Heat transfer in liquid fluidized beds with a concentric heater, Trans. Inst. Chem. Eng. 49 (1971) 196–203.
- [12] F.W. Dittus, L.M.K. Boelter, Heat transfer in automobile radiators of the tubular type, Publications in Engineering University of California Berkeley 2 (13) (1930) 443–461.
- [13] B.S. Petukhov, Heat transfer and friction in turbulent pipe flow with variable physical properties, Adv. Heat Transfer 6 (1970) 503–565.
- [14] V. Gnielinski, New equations for heat and mass transfer in turbulent pipe and channel flow, Int. Chem. Eng. 16 (1976) 359–368.
- [15] K. Muroyama, M. Fukuma, A. Yasunishi, Wall-to-bed heat transfer in liquid–solid and gas–liquid–solid fluidized beds Part I: liquid–solid fluidized beds, Can. J. Chem. Eng. 64 (1986) 399–408.
- [16] Y. Kang, L.T. Fan, S.D. Kim, Immersed heater-to-bed heat transfer in liquid–solid fluidized beds, AIChE J. 37 (7) (1991) 1101–1106.
- [17] N. Bošković-Vragolović, Analogija prenosa količine kretanja, toplote i mase u sistemima tečnost–čvrsto, Ph.D. Thesis, Faculty of Technology and Metallurgy, University of Belgrade, 2002.
- [18] K. Nakamura, C.E. Capes, Vertical pneumatic conveying: a theoretical study of uniform and annular flow models, Can. J. Chem. Eng. 51 (1973) 39–46.
- [19] Ž.B. Grbavčić, R.V. Garić, D.V. Vuković, Dž.E. Hadžismajlović, H. Littman, H.M. Morgan III, S.Dj. Jovanović, Hydrodynamic modeling of vertical liquid–solids flow, Powder Technol. 72 (1992) 183–191.
- [20] E. Barnea, J. Mizrahi, A generalized approach to the fluid dynamics of particulate systems-I. General correlation for fluidization and sedimentation of solids multiparticle systems, Chem. Eng. J. 5 (1973) 171–189.
- [21] R.V. Garić-Grulović, Ž.B. Grbavčić, Z.Lj. Arsenijević, Heat transfer and flow pattern in vertical liquid–solids flow, Powder Technol. 145 (2004) 163–171.
- [22] H.T. Chilton, P.A. Colburn, Mass transfer (Absorption) coefficient – prediction from the data on heat transfer and fluid friction, Ind. Eng. Chem. 26 (1934) 1183–1187.